J|A|C|S
ARTICLES
Published on Web 03/08/2005

Tuning the Orientation of an Antigen by Adsorption onto Nanostriped Templates

Antoine Pallandre, Benoit De Meersman, Françoise Blondeau, Bernard Nysten, and Alain M. Jonas*

Contribution from the Unité de Physique et de Chimie des Hauts Polymères (POLY) and Research Center in Micro- and Nanoscopic Materials and Electronic Devices (CeRMiN), Université catholique de Louvain, Place Croix du Sud, 1, B-1348 Louvain-la-Neuve, Belgium

Received October 19, 2004; E-mail: jonas@poly.ucl.ac.be

Abstract: We investigate the adsorption of a globular protein (P.69 pertactin, also known as antigen 69k) on protein-repellent hydrophilic substrates bearing regularly spaced hydrophobic nanostripes, for stripe widths comprised between 20 and 160 nm. Protein adsorption is shown to be remarkably well-controlled by the templating substrates, with a near-to-perfect reproduction of stripes by the protein monolayer down to 20 nm width, except for a 5−10 nm broadening. However, whereas the ellipsoidal protein forms a dense monolayer with random orientation of its long axis for large stripe widths, it adsorbs in a predominantly side-on (flat-on) orientation for stripe widths below 50 nm, due to the easier reorientation (interfacial relaxation) of the proteins adsorbed at the edges of the stripes, which experience a decreased lateral interaction. These results show that protein confinement in regions of a size similar to their dimensions can be used to tune their orientation, which may be of interest for applications in high-density sensor devices.

Introduction

Proteins are essential components of living systems, and the study of their interactions with other proteins or with surfaces is critical for basic biological research as well as for practical applications such as tissue engineering and biosensors for proteomics and medicine, etc. Therefore, a number of recent studies[1−8] have been devoted to the local deposition of proteins in domains of size typically in the 50−100 nm range or above. These studies are essentially motivated by the need to develop practical ways to fabricate high-density and high-throughput protein-based biosensing devices. In some cases, the proteins are directly transferred and reacted on surfaces by dip-pen nanolithography[1,3,8] or nanocontact printing.[5] In other examples, solutions of proteins are reacted with surfaces bearing binary chemical nanopatterns produced by scanning probe nanolithography[2,7] or by a another nanolithography such as nanoimprint.[6]

It is thus appropriate and timely to check the behavior of proteins when confined in domains of very small dimensions, which will be relevant for high-density sensor applications. In the present paper, we explore the adsorption of a typical globular protein onto alkane nanostripes drawn in a background of adsorption-resistant oligo(ethylene oxide). Such nanostructured surfaces were recently shown to control the conformations of charged synthetic polymer chains:[9] When the width of the adsorbing stripes decreases below the average end-to-end distance of the chains in solution, the conformations of the chains are strongly perturbed upon adsorption. This was revealed, e.g., by a 5-fold increase of the height of the stripes of repeatedly adsorbed macromolecules, as compared to the height measured after adsorption on unstructured homogeneous surfaces.

These results were obtained for polyelectrolytes in the so-called persistent regime, in which chains adopt a locally rigidified wormlike conformation, due to long-range repulsion between charged groups in water of low ionic strength. An intriguing question is, how would chains coiled in a much more compact way interact with such directing nanotemplates? One should expect compact macromolecular globules such as globular proteins to interact with surfaces similar to nanoparticles, with no or little conformational perturbation. However, the orientation and interfacial relaxation of such globular macromolecules now becomes a central issue, of strong relevance for practical applications. This is one of the issues addressed in the present paper.

Results and Discussion

The protein selected for this study is P.69 pertactin, a compact globular antigen. This antigen, also known as antigen 69k (from its apparent molar mass on gel), is located in the outer membrane

(1) Wilson, D. L.; Martin, R.; Hong, S.; Cronin-Golomb, M.; Mirkin, C. A.; Kaplan, D. L. *Proc. Natl. Acad. Sci. U.S.A.* **2001**, *98*, 13660−13664.
(2) Lee, K. B.; Park, S. J.; Mirkin, C. A.; Smith, J. C.; Mrksich, M. *Science* **2002**, *295*, 1702−1705.
(3) Renault, J. P.; Bernard, A.; Juncker, D.; Michel, B.; Bosshard, H. R.; Delamarche, E. *Angew. Chem., Int. Ed.* **2002**, *41*, 2320−2323.
(4) Lee, K.-B.; Lim, J.-H.; Mirkin, C. A. *J. Am. Chem. Soc.* **2003**, *125*, 5588−5589.
(5) Li, H.-W.; Muir, B. V. O.; Fichet, G.; Huck, W. T. S. *Langmuir* **2003**, *19*, 1963−1965.
(6) Hoff, J. D.; Cheng, L.-J.; Meyhöfer, E.; Guo, L. J.; Hunt, A. J. *Nano Lett.* **2004**, *4*, 853−857.
(7) Gu, J.; Yam, C. M.; Li, S.; Cai, C. *J. Am. Chem. Soc.* **2004**, *126*, 8098−8099.
(8) Bruckbauer, A.; Zhou, D.; Kang, D.-J.; Korchev, Y. E.; Abell, C.; Klenerman, D. *J. Am. Chem. Soc.* **2004**, *126*, 6508−6509.
(9) Pallandre, A.; Moussa, A.; Nysten, B.; Jonas, A. M. Submitted for publication.

10.1021/ja043656r CCC: $30.25

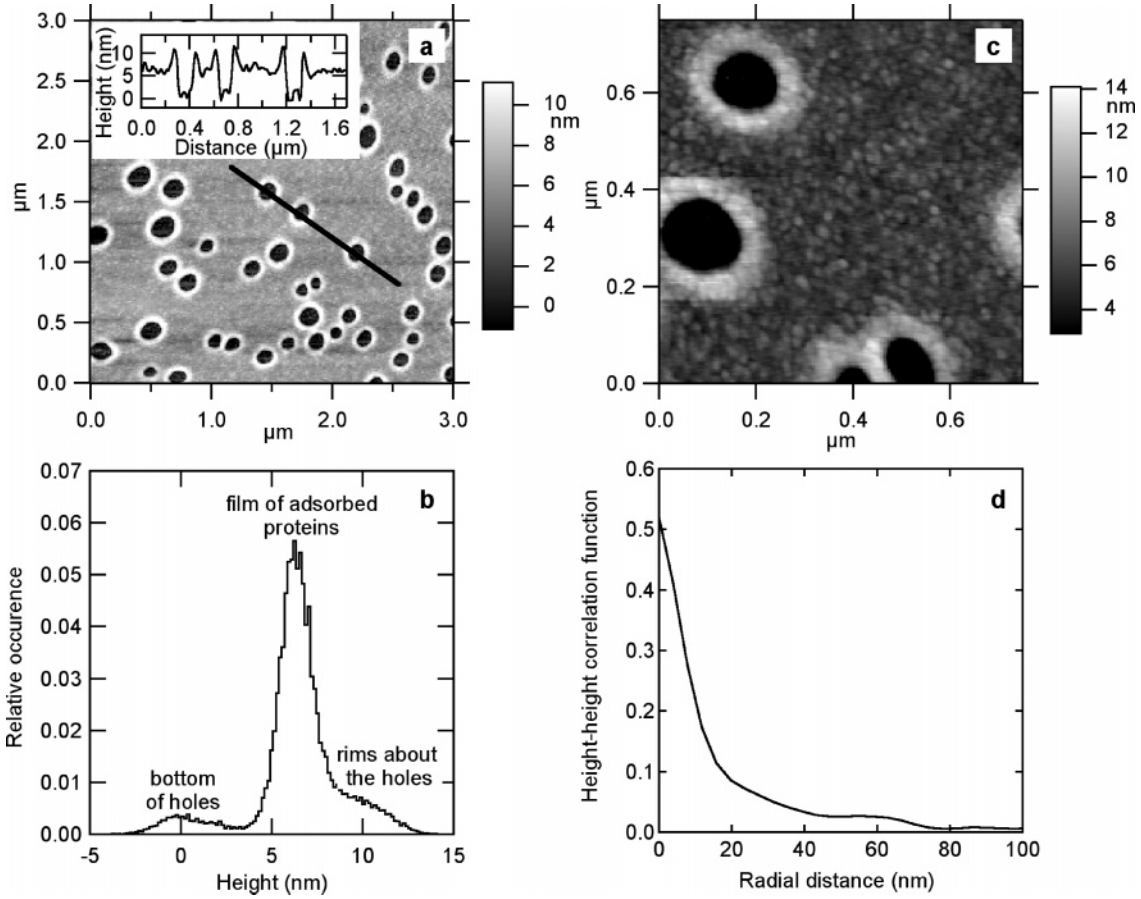

Figure 1. (a) AFM image (topography) of a layer of antigen 69k adsorbed on a homogeneous alkylsilanized silicon wafer, showing the onset of dewetting. The inset is a height profile along the black line in the image. (b) Histogram of the heights of the pixels in image a, from which the average height of the film is computed. (c) AFM image (topography) of the adsorbed protein layer showing individual macromolecules. (d) circular average of the height−height correlation function of regions of image c devoid of holes, allowing us to quantify the lateral size of the nodules.

of *Bordetella pertussis*. The protein is an essential component of acellular vaccines against whooping cough,[10−12] and its structure was determined by X-ray crystallography.[13] Pertactin bears the tripeptide Arg-Gly-Asp (RGD) motif, which is involved in protein−protein interactions to promote cell binding, and is slightly negatively charged at a pH above 5.7−6. The shape of P.69 pertactin is roughly ellipsoidal, with typical axis lengths of 10.6, 3.8, and 2.5 nm.[13] The substrates are similar to the ones reported before[14] and consist of (100) silicon wafers of 0.3 nm root-mean-square (rms) roughness, covered with parallel stripes of alkylsilane of varying width and of 250 nm repeat period, drawn in a background of oligo(ethylene oxide) silane. Details on the fabrication and characterization of the substrates were reported before.[9,14] The alkyl stripes should favor protein adsorption due to hydrophobic interactions in water, whereas the oligo(ethylene oxide) background is known to minimize protein adsorption in water.[15−17] The height difference between stripes and background is of the order of 0.1−0.2 nm only,[9] which guarantees that the oligo(ethylene oxide) molecules do not spill over the narrow hydrophobic stripes.

The antigen was first adsorbed on silicon wafers homogeneously silanized with the alkylsilane (see Experimental Section). The adsorbed layer was characterized in air after abundant rinsing in ultrapure water. A value of 6.8 nm was obtained by X-ray reflectometry (XRR) for the average thickness of the organic film on the silicon wafer. Considering that the thickness of the alkylsilane layer amounts to 0.9 nm,[14] the thickness of the adsorbed protein layer is 5.9 nm.

Atomic force microscopy (AFM) images of the adsorbed layer are presented in Figure 1. Randomly dispersed holes surrounded by a rim of accumulated material can be seen in the layer (Figure 1a), suggesting dewetting of the protein film by a mechanism of nucleation and growth of holes. Dewetting most probably occurs during drying, starting from surface heterogeneities, due to unfavorable van der Waals interactions in air between the hydrophobic silane and the protein. The presence of the holes should be considered as an asset, allowing easy determination of the film thickness by AFM. A value of 6.1 nm is obtained from the histogram of the pixel heights in the AFM image (Figure 1b), in good agreement with the 5.9 nm obtained by XRR.

(10) Podda, A.; Nencioni, L.; Marsili, I.; Peppoloni, S.; Volpini, G.; Donati, D.; Di Tommaso, A.; De Magistris, M. T.; Rappuoli, R. *Vaccine* **1991**, *9*, 741−745.
(11) Van Damme, P.; Burgess, M. *Vaccine* **2004**, *22*, 305−308.
(12) Gustafsson, L.; Hallander, H. O.; Reizenstein, E.; Storsaeter, J. *New Engl. J. Med.* **1996**, *334*, 349−355.
(13) Emsley, P.; Charles, I. G.; Fairweather, N. F.; Isaacs, N. W. *Nature* **1996**, *381*, 90−92.
(14) Pallandre, A.; Glinel, K.; Jonas, A. M.; Nysten, B. *Nano Lett.* **2004**, *4*, 365−371.
(15) Jeon, S. I.; Lee, J. H.; Andrade, J. D. *J. Colloid Interface Sci.* **1991**, *142*, 149−158.
(16) Harder, P.; Grunze, M.; Dahint, R.; Whitesides, G. M.; Laibinis, P. E. *J. Phys. Chem. B* **1998**, *102*, 426−436.
(17) Herrwerth, S.; Eck, W.; Reinhardt, S.; Grunze, M. *J. Am. Chem. Soc.* **2003**, *125*, 9359−9366.

Upon closer examination (Figure 1c), the layer appears to be made of nodules, whose average lateral diameter can be obtained from the self-correlation triangle of the circularly averaged height−height correlation function[18] computed over regions devoid of holes (Figure 1d). A value of about 20 nm is found for the average lateral diameter of the nodules, with some nodules having diameters as large as 30 nm. The roughness of the protein layer in regions devoid of holes is 0.7 nm, and the peak-to-valley height difference is ∼4 nm. Considering that the apex radius of curvature of the AFM tip is 10 nm, an object of 4 nm height would be broadened by 10−15 nm due to finite tip size (see Experimental Section). This value is an upper bound for the tip broadening effect and leads to average lateral dimensions for the nodules in the 5−20 nm range, in good agreement with the dimensions of P.69 pertactin molecules. The 6 nm average thickness, together with the 4 nm peak-to-valley differences of height, and the lateral size of the nodules in the 5−20 nm range support a model wherein the elongated ellipsoidal antigen macromolecules adsorb on the substrate with random orientations of their long axis.

In contrast, the average height of the rim of proteins collected around the holes is about 10 nm (Figure 1b), close to the longest dimension of P.69 pertactin. This suggests that the film of proteins slowly dewets by collecting molecules in rims of close-packed, end-on molecules, surrounding empty holes. Different postadsorption events and interfacial relaxation processes have been reported for proteins, including slow clustering,[19,20] spreading-induced conformational changes (partial denaturation),[21−24] and reorientation,[24−27] depending on the nature of the surface and on the type of proteins, hard or soft. In the present case, clustering and reorientation appear to be the dominant post-adsorption relaxation mechanisms of P.69 pertactin, when dried in air.

Adsorption experiments were then performed on alkyl/oligo(ethylene oxide) nanopatterns. Figure 2a presents the topography obtained without application of a rinsing step. The proteins are seen to adsorb on the whole surface, with however a much higher density of macromolecules adsorbed on the hydrophobic alkylsilane dots than on the hydrophilic oligo(ethylene oxide) background, resulting in a height difference of 2.5−3 nm. The contrast between hydrophobic and hydrophilic regions can be increased by applying a rinsing step after adsorption, as shown in Figure 2b−f, although some limited contamination of the oligo(ethylene oxide) background still remains. The most striking observation is that adsorption reproduces remarkably well the features of the underlying directing templates, down to very small stripe widths. In addition, it can be noticed that stripes wider than 90 nm display features typical of the proteins adsorbed onto a homogeneous monolayer of alkylsilane, namely, the appearance of small holes suggesting the onset of dewetting. Less wide lines do not exhibit holes but are slightly discontinuous.

The quantitative evaluation of antigen adsorption is summed up in Figure 3. The width of stripes of the antigen is seen to follow the width of the underlying alkylsilane stripes, except for a constant broadening of 20 nm (Figure 3b). The main part of this broadening (10−15 nm) arises from dilation of the stripes by the AFM tip (see Experimental Section); the remainder should be attributed to the finite size of the macromolecules. Contrarily to the case of synthetic polyelectrolytes reported before,[9] no saturation of the stripe width of adsorbed macromolecules can be observed, down to 20 nm alkyl stripe width. This results from the more compact shape of the protein as compared to the more extended synthetic polyelectrolytes in water, which allows proteins to follow easily very narrow templating tracks.

The height of the adsorbed stripes is reported in Figure 3a versus stripe width. Here again, the behavior is distinctly different from the one reported for the synthetic polyelectrolytes.[9] Whereas the height of the stripes of synthetic polyelectrolyte chains increased upon reduction of the stripe width, due to folding of the chains at the edges of the templating stripes, the height of the protein lines actually decreases when the stripe width decreases below 50 nm. For lines wider than 50 nm, the height is identical to the one obtained on homogeneous surfaces.[28]

On the narrower stripes, the protein layer is 3−3.5 nm high, which corresponds to a layer of P.69 pertactin molecules adsorbed in a side-on (or flat-on) orientation (i.e., the direction of the long axes of the ellipsoidal proteins are parallel to the surface). By contrast, stripes wider than 50 nm have a height (6 nm) corresponding to an isotropic distribution of directions for the long axis of the macromolecules. These differences of height are significant, and do not arise from experimental artifacts, since the same experimental conditions were applied for all samples. Furthermore, the low spring constant of the cantilevers and the soft-tapping conditions used to perform the AFM imaging minimize potential damages to the soft protein layers, as confirmed by the good agreement obtained by AFM and XRR for the thickness of the protein layer on homogeneously hydrophobized wafers. Thus, we may safely conclude that the observed differences simply result from different orientations of the proteins, which vary between random and side-on depending on stripe width.

The variation of protein orientation with stripe width may be understood by considering the interfacial relaxation of proteins after adsorption. When proteins adsorb on a surface, the final surface coverage depends on the ratio between the adsorption rate and the interfacial relaxation rate of adsorbed molecules, which relax by clustering, spreading, or reorienting as mentioned above.[19−27] Faster adsorption rates lead to protein layers of higher packing density in shorter adsorption times. The ensuing increased lateral steric hindrances between neighboring molecules decrease the probability of interfacial relaxation, ultimately leading to a larger final surface coverage since

(18) Haubruge, H. G.; Gallez, X. A.; Nysten, B.; Jonas, A. M. *J. Appl. Crystallogr.* **2003**, *36*, 1019−1025.
(19) Calonder, C.; Tie, Y.; Van Tassel, P. R. *Proc. Natl. Acad. Sci. U.S.A.* **2001**, *98*, 10664−10669.
(20) Tie, Y.; Calonder, C.; Van Tassel, P. R. *J. Colloid Interface Sci.* **2003**, *268*, 1−11.
(21) Norde, W.; Giacomelli, C. E. *Macromol. Symp.* **1999**, *145*, 125−136.
(22) Wertz, C. F.; Santore, M. M. *Langmuir* **1999**, *15*, 8884−8894.
(23) Pancera, S. M.; Alvarez, E. B.; Politi, M. J.; Gliemann, H.; Schimmel, Th.; Petri, D. F. S. *Langmuir* **2002**, *18*, 3517−3523.
(24) Wertz, C. F.; Santore, M. M. *Langmuir* **2002**, *18*, 706−715.
(25) Robeson, J. L.; Tilton, R. D. *Langmuir* **1996**, *12*, 6104−6113.
(26) Wertz, C. F.; Santore, M. M. *Langmuir* **2002**, *18*, 1190−1199.
(27) Daly, S. M.; Przybycien, T. M.; Tilton, R. D. *Langmuir* **2003**, *19*, 3848−3857.

(28) For one sample (Figure 2f, and data point in parentheses in Figure 3), the grooves between the protein stripes were too narrow to allow complete penetration of the AFM tip, resulting in an inaccurate determination of the height of the stripes.

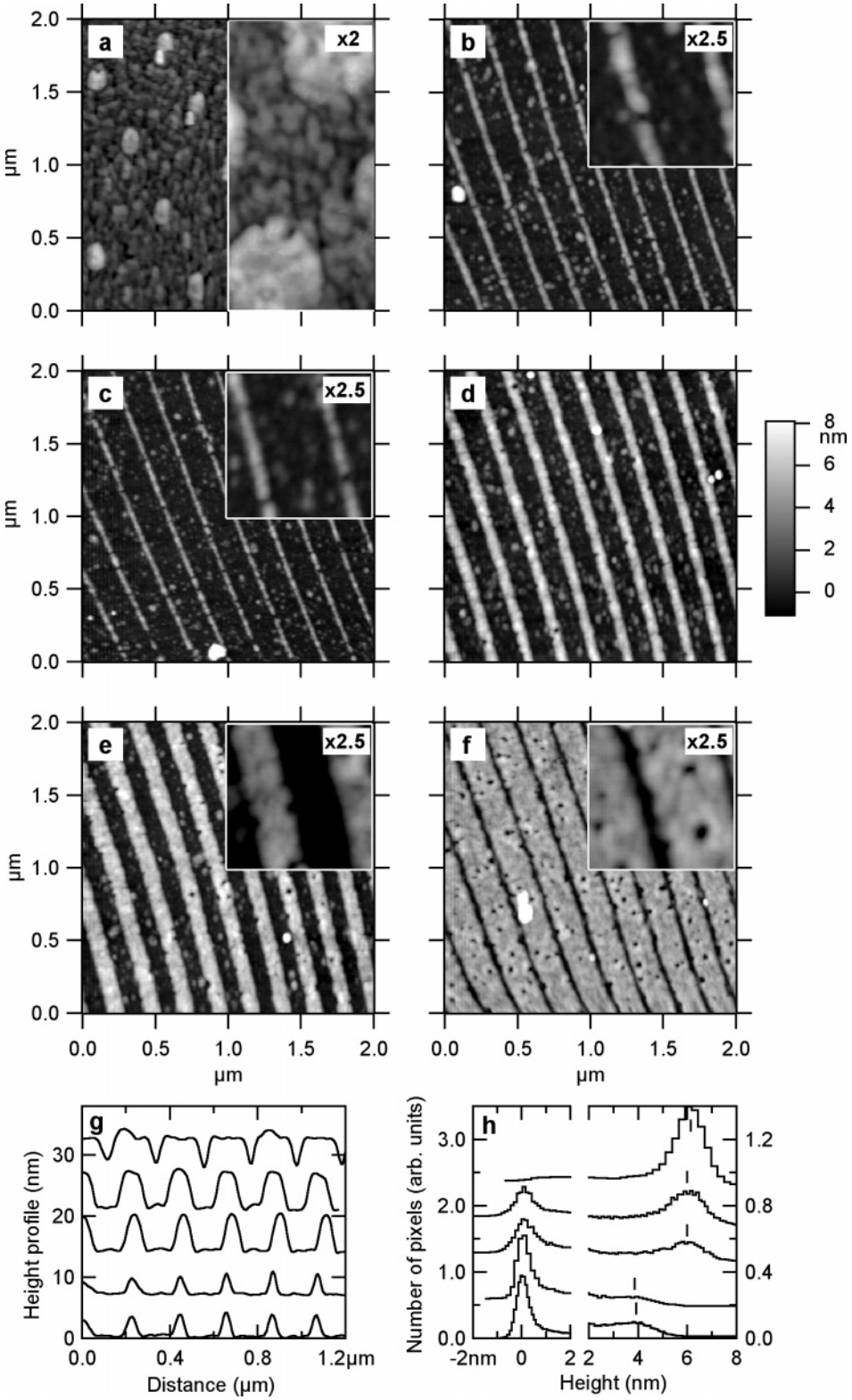

Figure 2. (a) AFM images (topography) of antigen 69k adsorbed onto alkylsilane dots of 150 (left) and 350 nm (right) diameter, drawn in a background of oligo(ethylene oxide), without application of a rinsing step. (b−f) AFM images (topography) of antigen 69k adsorbed on alkylsilane stripes of 20 (b), 35 (c), 55 (d), 90 (e), and 170 nm (f) width, drawn in a background of oligo(ethylene oxide), with application of a rinsing step. The repeat period of the stripes is 250 ± 10 nm. (g) Average height profiles computed along lines drawn perpendicularly to the stripe direction for, from bottom to top, images b−f. The averaging was performed over 1 μm distance along the stripes. For the trace corresponding to image f, limited penetration of the tip into the grooves prevents an accurate determination of the height of the stripes. Traces are displaced vertically by increments of 7 nm. (h) Histograms of the height of the pixels for, from bottom to top, images b−f. The first peak originates from the background pixels, whereas the second peak is due to the pixels belonging to the stripes of adsorbed proteins. The histograms are shifted vertically for clarity.

interfacial relaxation processes usually result in larger projected areas for proteins.

In the present case, however, the adsorption rates are not expected to vary from experiment to experiment. Indeed, recent

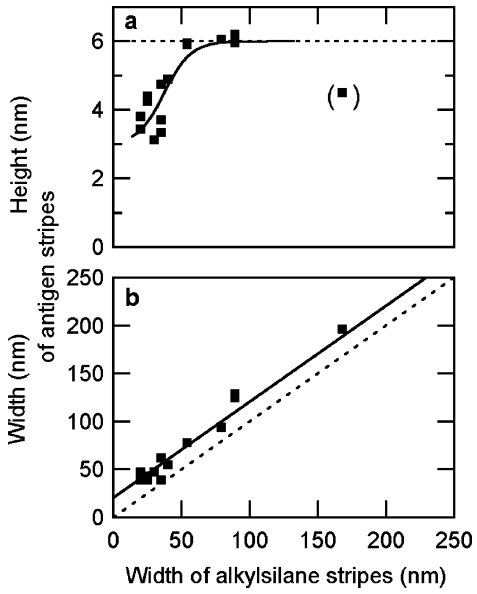

Figure 3. (a) Variation of the height of the stripes of adsorbed antigens with the width of the templating alkylsilane stripes (repeat period of the stripes, 250 nm). Data points between parentheses are erroneous due to limited penetration of the AFM tip in narrow grooves. The dashed line indicates the thickness of an antigen layer adsorbed onto an homogeneous alkylsilanized substrate. The continuous line is a fit to a sigmoidal function. (b) AFM-determined width of antigen stripes versus the width of the templating alkylsilane stripes. The dashed line corresponds to equal stripe widths. The continuous line is a linear fit to the data. The antigen stripes appear on the average 20 nm wider than the original alkylsilane templating stripes, due in part from dilation of the stripes by the AFM tip (which accounts for 10−15 nm) and in part from the finite size of the antigen.

previous works on the adsorption of proteins and other macromolecules[29−31] on nanoheterogeneous random binary surfaces indicate that the initial adsorption rate does not depend on the chemical composition of the surfaces, except when long-range forces such as electrostatic repulsion are introduced in the system.[31] Therefore, another reason is required to explain the varying surface coverage observed on nanostriped templates. The decreased lateral interaction experienced by macromolecules at the edges of the stripes is an obvious factor favoring protein reorientation. As shown previously, the oligo(ethylene oxide) background tolerates limited protein adsorption. Therefore, the extra space left open at the edges of the stripes allows for the relaxation of border proteins, which, in turn, favors the reorientation of their direct neighbors in a kind of "domino effect". The spatial extent of this effect will be limited to a few neighboring macromolecules only: in the present case, the effect is only significant for stripe widths below 50 nm, which corresponds to about 10 proteins only. This demonstrates that the orientation of proteins may be controlled by confinement into regions of sizes close to their dimensions, which opens interesting possibilities for applications in the field of high-density protein sensors.

Conclusions

To conclude, our experiments demonstrate that compact globular proteins can be selectively and locally adsorbed down to extremely small dimensions, about twice their longer dimension, which is of interest for applications in the field of high-density biosensors. In addition, their orientation can be tuned by reducing the size of the adsorbing regions below 50 nm, due to the easier reorientation of the proteins adsorbed at the edges of the stripes, which experience a decreased lateral interaction. Our results also point to significant differences in adsorption behavior with synthetic polyelectrolytes, illustrating the complex interplay between pattern size and macromolecular conformation in solution. These differences of behavior suggest that, by playing with pattern sizes and shapes, an unprecedented control could be attained over macromolecules at the nanoscale, provided the pattern is tuned to fit with the nature of the macromolecules.

Experimental Section

Materials. P.69 pertactin was provided by GlaxosmithKline Biologicals (Rixensart, Belgium), and was stored in phosphate buffer at pH 7.6 (20 mM of K_2HPO_4/KH_2PO_4 and 0.5 M of NaCl in 50/50 (v/v) water/glycerol mixtures), at the concentration of 211 μg/mL. All silanes were obtained from Gelest and used as received, after storage under dry argon. One-side-polished silicon wafers of 475 μm thickness were obtained from ACM (Applications Couches Minces, France) with (100) orientation. The fabrication of striped nanopatterns on these wafers is described elsewhere.[9,14] The width of alkylsilane stripes was estimated by measuring by scanning electron microscopy the widths of Ti stripes realized by Ti lift-off on lithographied masks identical to the ones used for the silanation.

Antigen Adsorption. A droplet of the antigen solution was placed for 1 h at room temperature onto patterned silicon wafers. The sample was then abundantly rinsed under flowing ultrapure water for 2 min, before AFM observations.

Atomic Force Microscopy. AFM images were recorded in air with an Autoprobe CP from Thermomicroscopes using a 5 μm scanner. The images were recorded in intermittent-contact mode (IC-AFM), using Pointprobe "Force Modulation" sensors (Nanosensors). These cantilevers have a resonance frequency around 60−70 kHz, a typical spring constant of about 3 N/m, and an integrated Si tip with a tip apex radius of curvature of about 10 nm. Soft-tapping conditions were used throughout the work; i.e., the ratio between the set-point amplitude and the free amplitude of the cantilever vibration was always kept above 0.85. These imaging conditions and the relatively low spring constant of the used cantilevers minimize the indentation of the tip in the soft protein layer and avoid damage to the layer.[32] A first- or second-order flattening procedure (line by line) was performed on AFM images before analysis.

Image Treatment and Analysis. The average height of the stripes of adsorbed antigen was computed from the height histogram of the images. Bimodal histograms were obtained in all cases, with the first and second maxima corresponding to the height of the background and of the antigen stripes, respectively. The width of the stripes was computed by methods reminiscent of the ones used for the analysis of the scattering by lamellar systems.[18−34] In short, the autocorrelation $C_2(x,y)$ of the image $I(x',y')$ was first computed; then, a one-dimensional correlation function $C_1(r)$ was obtained along a line passing through the origin, in the direction perpendicular to the stripes. The second derivative of $C_1(r)$ provided an interface distribution function $F_1(r)$, whose first two maxima correspond to the width of the stripes and interstripe gaps, respectively. Sharp maxima testified for the limited distribution of widths of the stripes. For images of the protein monolayer

(29) Chun, K.-Y.; Huang, Y.-W.; Gupta, V. K. *J. Chem. Phys.* **2003**, *118*, 3252−3257.
(30) Huang, Y.-W.; Chun, K.-Y.; Gupta, V. K. *Langmuir* **2003**, *19*, 2175−2180.
(31) Huang, Y.-W.; Gupta, V. K. *J. Chem. Phys.* **2004**, *121*, 2264−2271.
(32) Behrend, O. P.; Odoni, L.; Loubet, J.-L.; Burnham, N. A. *Appl. Phys. Lett.* **1999**, *75*, 2551−2553.
(33) Stribeck, N. *J. Appl. Crystallogr.* **2001**, *34*, 496−503.
(34) Haubruge, H. G.; Jonas, A. M.; Legras, R. *Macromolecules* **2004**, *37*, 126−134.

obtained on homogeneous alkylsilanized wafers, a bi-dimensional correlation function was computed as described previously[18] and then averaged circularly to obtain a one-dimensional correlation function. The width at the base of the peak centered about the origin, i.e., the so-called self-correlation triangle, was taken as an estimate for object size.

A higher bound for dilation effects due to the finite apex radius of curvature R of the AFM tip was estimated as follows. If the height profile of the multilayer stripes were a square pulse of height h and width w, the image would be a pulse of h with convex rounded sides mirroring the shape of the apex of the tip. The width at the base of this broadened pulse is $w + 2(h(2R - h))^{0.5}$, and the width of its upper side is w. Since the interface distribution function is the autocorrelation of the first derivative of the height profiles,[33,34] it will present peaks for distances between two spatial locations where the first derivative of the height profile is maximum. For the case of our rounded pulses, this will be the case for distances corresponding to the widths of the base of the broadened pulses. Analysis of this profile by the interface distribution function would thus provide a width of about $w + 2(h(2R - h))^{0.5}$. The experimental broadening was thus computed for all samples, on the basis of the known height of the stripes, taking $R = 10$ nm. An average value of 16 nm was obtained (standard deviation, 1.5 nm). This is a higher bound for the experimental broadening, since profiles varying less steeply than a square pulse will be less affected by dilation effects, leading us to estimate the broadening to be in the range of 10−15 nm.

Acknowledgment. We are indebted to Paul Rouxhet, Vincent Bayot, and Jean-Pierre Raskin for providing access to experimental facilities, to Sophie Demoustier-Champagne for discussions, and to Gaëtane Metz (GlaxosmithKline) for providing us with antigen 69k. This research was supported by the DG Scientific Research of the French Community of Belgium (Action de Recherche Concertée 00/05-261 "NANORG"), by the Belgian Fund for Fundamental Collective Research (FRFC), and by the Belgian Federal Science Policy (IAP network "Supramolecular Chemistry and Supramolecular Catalysis"). B.N. is a Research Associate of the Belgian Fund for Scientific Research (FNRS).

JA043656R